Iran J Sci Technol Trans Sci (2021) 45:1843–1850
https://doi.org/10.1007/s40995-021-01160-x

RESEARCH PAPER

Growth, Characterization and NLO Property Study of Doped L-Alanine Crystal

M. R. Hareeshkumar[1] · G. J. Shankaramurthy[1] · A. Alhadhrami[2] · M. R. Jagadeesh[3] · B. M. Prasanna[4]

Received: 23 March 2021 / Accepted: 5 June 2021 / Published online: 5 July 2021

Abstract
L-Alanine (LA) is a promising nonlinear optical material from the amino acid category. The results of thorough deliberations on physiochemical and optical properties of pure and mixed forms of LA attracted many researchers. In this context, ammonium bromide added LA crystals were grown by solvent evaporation process and they were analyzed through various characterization tools. The orthorhombic crystal system and the slight intensity variation were noticed by diffraction studies. The vibrational lines of diverse functional groups and element identification were made by FT-IR and EDAX analysis, respectively. The optical properties were evaluated to witness the transparency to the visible light along with UV lower limiting wavelength of 245 nm. The surface topography and melting point were analyzed through SEM and thermal studies, respectively. Mechanical behavior was examined through hardness test. The crystal under study has shown improved second harmonic generation efficiency compared to pure LA as revealed by Kurtz powder method.

Keywords Slow evaporation · Optical properties · Thermal properties · NLO properties

1 Introduction

Since the discovery of NLO phenomenon by Franken et al., continuously efforts are being made to search and design novel materials by many researchers with interdisciplinary emphasis. This led to ascertain the true potential of massive organic, inorganic and hybrid materials. Each of these classes of materials is unique in characteristic properties which incited for device applications (Franken and Hill 1961; Wang et al. 1999; Ding et al. 2000). The research responsive readiness of different growing mechanisms and parallel inventions on new-fangled molecular architecture materials boosted the growth of single crystals and made nonlinear optics ever active in the scientific literature. In materials perspective, organics have the significant molecular flexibility but meager material stability whereas in inorganics NLO effect is bulk with noticeable stability. As a result, these consequences shifted the focus of the researchers to combine the favorable properties of these potential materials to frame organo-inorganic hybrid materials also called as semi organic materials. These materials have the proven nonlinearity, marginal angular sensitivity and better hardness. But, in metal organic coordination complexes, the organic ligand will influence the NLO and dielectric effect. Among various class of organic NLO materials, amino acids and their derivatives were treated exclusively due to their comprehensive features such as, zwitterionic nature providing the material hardness, ground state charge symmetry due to the presence of amino group for protonation and carboxylic group for deprotonation, etc. These intrinsic properties of amino acids engendered the possibilities to custom them for device applications. LA is a nonpolar alpha amino acid which fit into orthorhombic crystal system. The structural

✉ M. R. Hareeshkumar
hari.melgiri@gmail.com

[1] Department of Physics, UBDT College of Engineering, Davanagere, Constituent College of VTU, Belagavi, Karnataka 577004, India

[2] Department of Chemistry, College of Science, Taif University, P. O. Box 11099, Taif 21944, Saudi Arabia

[3] Department of Physics, Jain Institute of Technology, Davangere, Affiliated to VTU, Belagavi, Karnataka 577003, India

[4] Department of Chemistry, Jain Institute of Technology, Davangere, Affiliated to VTU, Belagavi, Karnataka 577003, India

organization and π–π* transitions of the carboxylic group makes LA optically active. Starting from the early efforts on crystallization of LA by H. J. Simpson et al. and L. Mosoguti et al. (Simpson and Marsh 1966; Misoguti et al. 1996) in 1966 to the present, there have been several momentous reports on LA derivatives which influenced researchers to focus on improving the comprehensive properties of LA (Rajan Babu et al. 2002a; Krishnakumar and Nagalakshmi 2006; Shanthi et al. 2014; Suresh 2020). In this context, many organic acids and inorganics were examined with LA in various proportions and as a result there is a substantial enhancement in its physiochemical properties which led to the tuned design in the molecular level to fabricate materials for applications such as opto-electronic, data storage, etc. Many ammonium salts were admixtured with well-known NLO materials to enhance the inclusive properties. In continuance, for the present study single crystals of ammonium bromide added with LA were obtained by solvent evaporation method and are subjected to various characterizations and the results are discussed.

2 Experimental Procedure

With the intent of growing single crystals by generating difference in evaporation rate of solute and solvent, the solvent evaporation process was employed. The crystal under study was primed with AR grade 1 mol percentage of ammonium bromide added to LA. Firstly, the intended quantity of LA was taken to make its solution from distilled water. Later, an equivalent quantity of ammonium bromide was leisurely added along with constant stirring to attain the solution homogeneity. Further, we kept the beaker in appropriate atmosphere for the growth with proper shielding of porous lid. On the lid we pricked (Bernal 1931; Rajan Babu et al. 2002b; Jaikumar et al. 2009; Lydia Caroline et al. 2011; Neelam Singh and Singh 2008; Dhanuskodi and K. 2004) holes for the solvent evaporation. After 26 days, crystals with the dimensions of 12 × 7x3 mm^3 were obtained and are shown in Fig. 1.

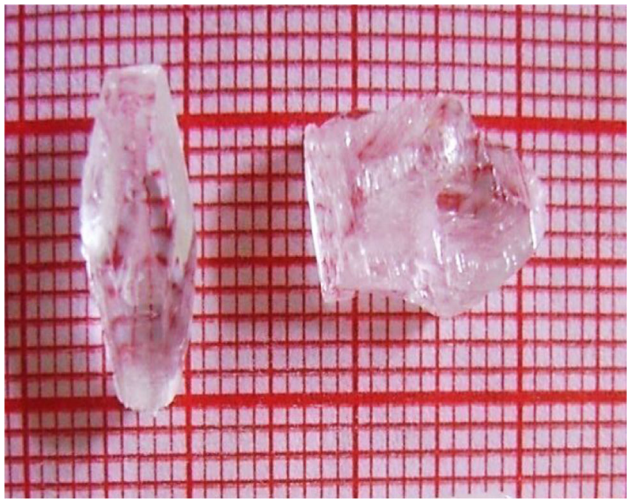

Fig.1 As grown single crystal

3 Results and Discussions

3.1 Diffraction Studies

The X-ray crystal diffraction studies were made using a Bruker smart Apex diffractometer and confirmed the orthorhombic crystal system with the cell parameters $a = 5.89$ Å, $b = 6.15$ Å, $c = 12.57$ Å, $\alpha = \beta = \gamma = 90°$ and the cell volume is $V = 455Å^3$. However, Pure L-alanine lattice parameters are $a = 6.302$ Å $b = 12.343$ Å $c = 5.78$ Å and the volume is $449Å^3$. The addition of dopant ensued in marginal modifications in the crystal parameters and cell volume (Bernal 1931). Further, the sample was made to fine powder by crushing and taken to powder X-ray diffractometer with Cu- Kα radiation with the wavelength of 1.5418 Å through 2θ scan (speed of 2° per minute) made between 10° to 80°. Figure 2 depicts the diffraction pattern which show well crystallinity. Further, it can be seen that the all the peaks were indexed and no peak left out un-indexed which specifies the absence any additional phases. The alteration in the peak position and intensity modifications confirms the active role of the dopant in the host lattice without altering its crystal system.

3.1.1 Williamson-Hall (W–H) method

By applying the W–H method for the powder diffraction pattern, the crystallite size and the strain were evaluated.

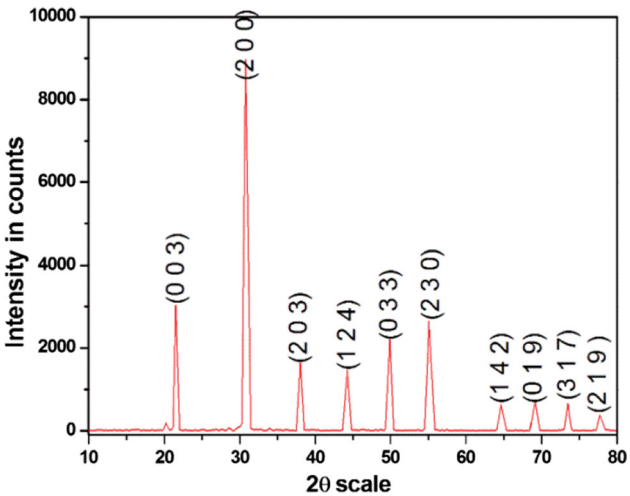

Fig.2 Powder X-ray diffraction pattern

For the experimental diffracted peaks full width half maxima (FWHM) is measured to the Gaussian shape to calculate the crystallographic distortion in terms of Lorentz intensity distribution according to the equation

$$\beta \cos\theta = \frac{K\lambda}{D} + 4\eta \sin\theta$$

where β is the FWHM of intense peaks, D is the crystalline size, θ is the position of the peaks, K is the Debye Scherrer value which is 0.94 for the spherical materials and λ is the X-ray wavelength. Plot a graph of $\beta\cos\theta$ against $4\sin\theta$ to obtain crystalline size and lattice strain is considered from the intercept and the resulting slope is shown in Fig. 3

From the slope, the strain value is about 5.641×10^{-4} with the crystalline size of 93.126 nm. The reduction of peak intensity and increment of FWHM diffraction peak indicates the lattice strain due to the dopant. In W–H plot, if the mechanical strain is positive it is to be considered as vacancy type point defects if it is negative then it corresponds to interstitial type point defects. Hence, the sample under study will be having some point defects which may be due to growth conditions.

3.2 FT-IR Spectral Analysis

The functional groups identification through FT-IR spectrometer (Thermo Nicolet, Avatar 370) in the range 4000–400 cm^{-1} was made and is as in Fig. 4. In energy side, the wide peak at 3089.29 cm^{-1} refers toward the O–H stretching vibrations and carbonyl stretch of C = O is identified with intense peak at 1617.99 cm^{-1}. In the overtone region, the major peak at 2111.37 cm^{-1} is due to combination of asymmetrical NH_3^+ bending (1618.74 cm^{-1}) and torsional oscillation of NH_3^+ (537.80 cm^{-1}). It is noticed that the stretching C = O of carboxylic acid and asymmetrical NH_3^+ bending vibration are in the same regime. The bending modes of CH_3 are vibrating at 1360.5 cm^{-1}. This study indicates protonation

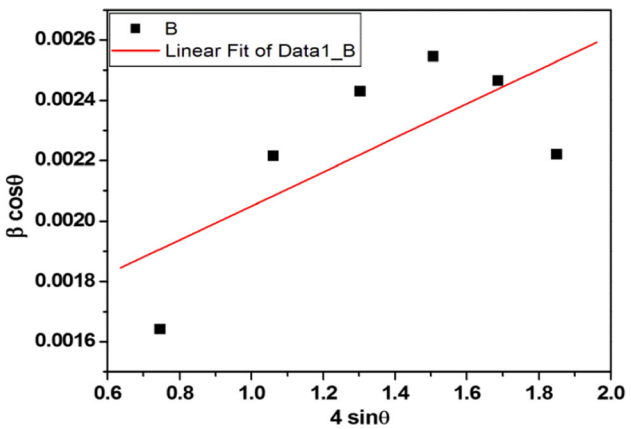

Fig.3 Plot $\beta\cos\theta$ versus $4\sin\theta$

of alanine carboxyl group by ammonium bromide. The protonation of LA by the dopant can be noticed between 918 and 1150 cm^{-1} asymmetrical coupled vibration which led to the confirmation of dopant in LA matrix. The tentative assigned functional groups are listed in Table1.

3.3 Optical Absorbance Studies

To be a germane NLO material, the range of optical transmittance and its cutoff wavelength values plays a vital role. UV–Visible involves preferment of the electron in σ and π orbital from lower to higher states. Hence, recording of UV–Vis spectrum is made with Varian Cary 5E spectrophotometer from 200 to 1500 nm and the spectrum is shown in Fig. 5a. Further, form the optical absorbance and transmittance data, the optical features such as energy gap, refractive index and susceptibility of the grown crystals were determined with the following relations to know the potentiality of the grown crystal.

It is seen that, in the considered wavelength range there is no noticeable light absorption along with widened transparency from 300 to 1500 nm is observed and it propose for various optical applications. The lower limiting value of wavelength is 245 nm and this is adequate for applications in the blue regime and particularly for harmonic generation of laser light.

The absorption coefficient (α) generally determines the light penetration by a material before it gets absorbed. The reliance of absorption coefficient on light energy (hν) given by Tauc's relation $\alpha h\nu = A(h\nu - Eg)^n$ which helps to understand the energy gap (Eg) of the crystals. Here, A is a constant and n is an index which determines the optical transition nature, i.e., indirect transition (n = 2) and direct transition (n = ½).

The direct band gap is calculated by plotting $(\alpha h\nu)^2$ versus photon energies hν (Fig. 5b) and it is 5.05 eV which signifies that the grown crystal has more light energy absorption for harmonic generation. It is observed that the energy gap value is decreased marginally upon doping compared to pure LA. However, this value is much appreciable when compared to other LA derivatives (Rajan Babu et al. 2002b; Jaikumar et al. 2009; Lydia Caroline et al. 2011; Neelam Singh and Singh 2008). Further, the photon energy can influence both crystal extinction coefficient and its refractive index which represents materials competence in device applications. Hence, the refractive index can be evaluated using the equation

$$\frac{n^2 - 1}{n^2 + 2} = 1 - \sqrt{\frac{E_g}{20}}$$

and is found to be 1.9. Further, by using this value the fraction of light reflected as a function of wavelength was

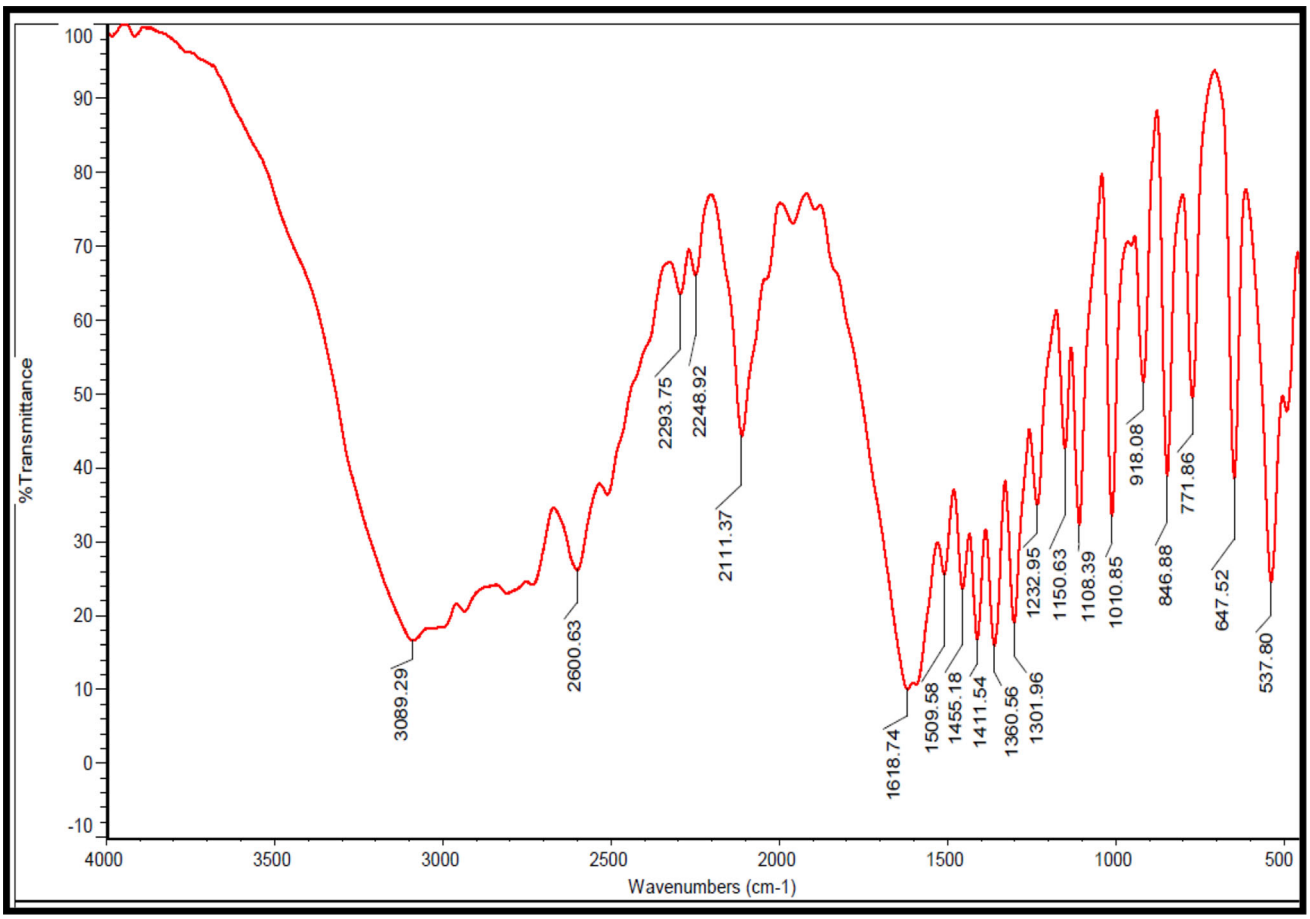

Fig.4 Recorded FT-IR spectra

Table 1 Functional group assignments

Wave number (cm^{-1})	Functional group
3089.29	O–H stretching
1617.99	Carbonyl stretch of C = O
2111.37	Asymmetrical NH_3^+ bending
1360.5	Bending modes of CH_3
1150	Asymmetrical coupled vibration
918	Protonation of LA

estimated using the equation $R = \frac{(n-1)^2}{(n+1)^2}$ and the calculated optical reflectance is found to be 0.11 in the transmission range. These optical parameters used in obtaining the susceptibility by taking refractive index equivalence with material relative permittivity for organic based NLO materials through the equation $\chi_c = \in_r -1$ or $\chi_c = n^2 - 1$. The calculated value is found to be 2.9. This high values suggests the material flexibility to respond to the applied field. These values suggests that the crystal could be suitable device applications.

3.4 Thermal Studies

The observation of thermal behavior of crystal was made by simultaneous thermo gravimetric (TGA) and differential thermal analysis (DTA) which was made in the presence of nitrogen and rate of heating being 10 °C per minute starting from room temperature to 800 °C. The preliminary taken sample mass was 15.855 mg.

From Fig. 6, the TGA curve evidently showing the solitary stage of dissociation. Initially, no weight loss up to 200 °C and the material begins to decompose from 210 °C. Further, it continues up to 270 °C. The quick weight loss between the 210 °C and 280 °C is due to complete dissociation of sample. The sharp endothermic peaks in DTA curve indicating the good order for crystalline nature and sample purity. These curves are observed at 274.17 °C, which correspond to melting point of the grown crystal. In the thermogram, neither there is endothermic nor does an exothermic peak which elucidates the absence phase

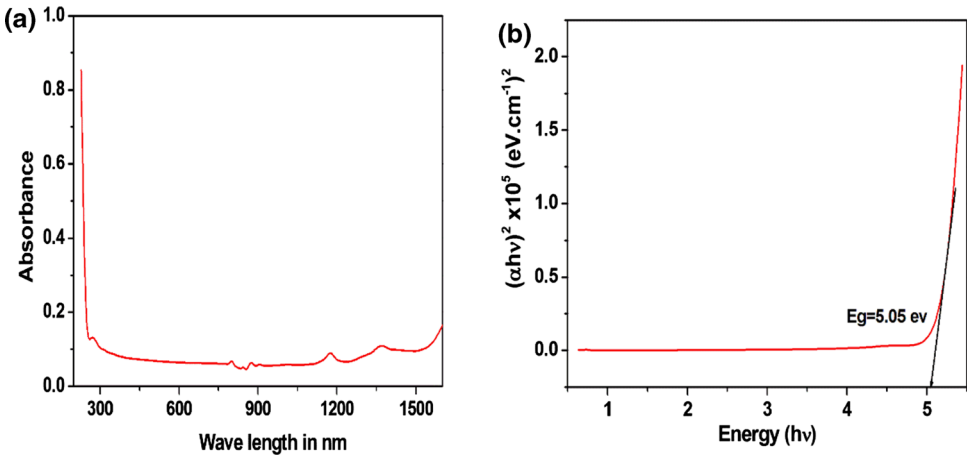

Fig. 5 **a**. Optical absorbance spectra and **b**. Tauc's plot

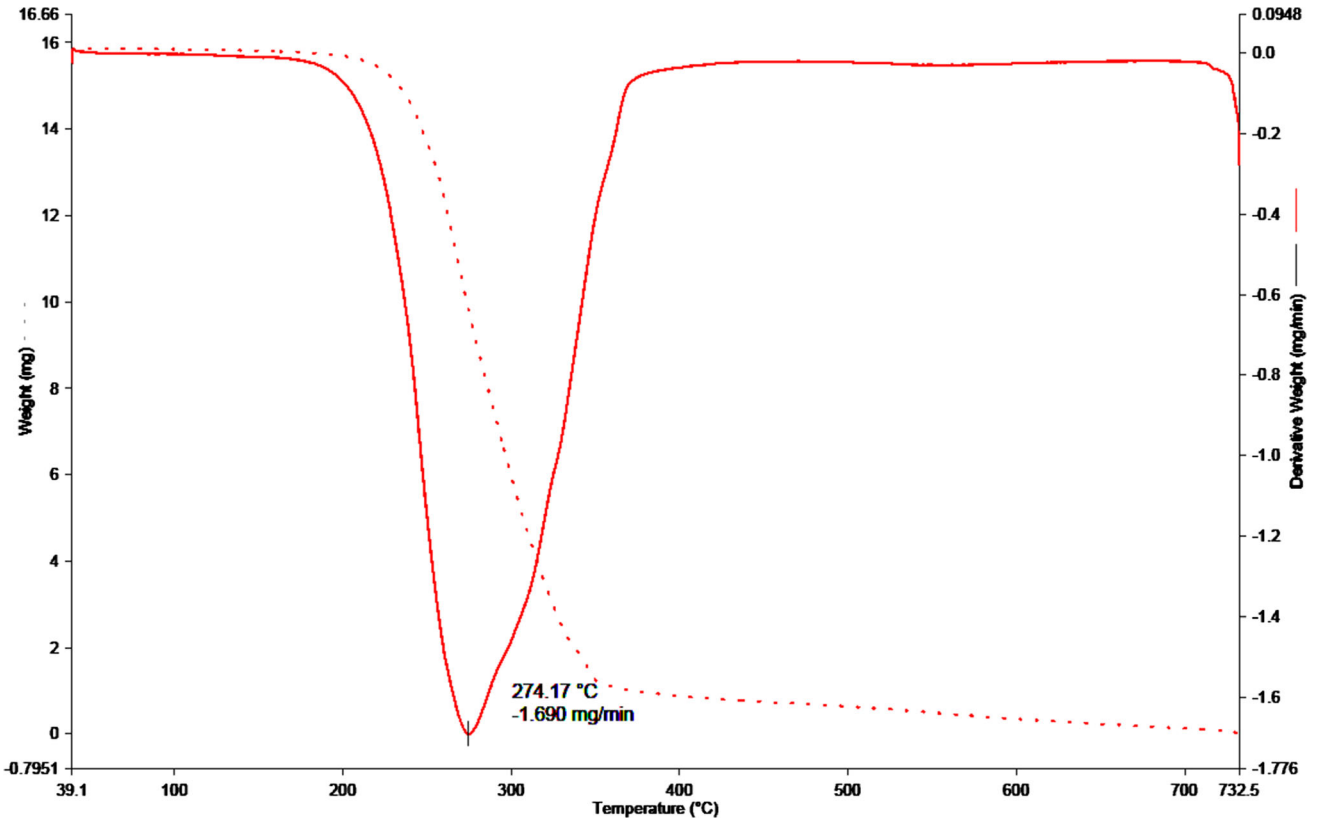

Fig.6 TG/DTA thermograms

transition prior to decomposition point. Hence, in conclusion, the grown crystal is stable and can be utilized for device application up to 274.17 °C. the dissociation temperature of some of the LA derivatives are listed in Table 2.

3.5 SEM and EDAX Studies

To examine the crystal topographical features and morphology the SEM study was done with JEOL JSM-6390LV model. The resulted image is as in Fig. 7, and it shows smooth surface having few inclusions showing the limited accommodation for the dopant in the LA crystalline matrix.

The compositional inference about elements or chemicals in the crystal was look over through EDAX spectrometer which is resulted from electron back scattering from the sample. Further, the resulted spectrum (energy v/s X-rays count) gives information about presence of elements in the sample in qualitative as well as quantitative manner. Figure 7 depicts the EDAX spectrum wherein the dopant presence may be observed.

Table 2 Melting point values of some of the reported L-alanine derivatives

Name of the L-alanine derivative	Melting point value (°C)
Pure LAL (Misoguti et al. 1996)	297
LAAB (Present work)	274
L-alaninium oxalate (Arun. 2009)	197
L-alanine DL Malic acid (Jaikumar et al. 2009)	224
L-alanine admixtured with perchloric acid (Jothi mani et al. 2015)	296

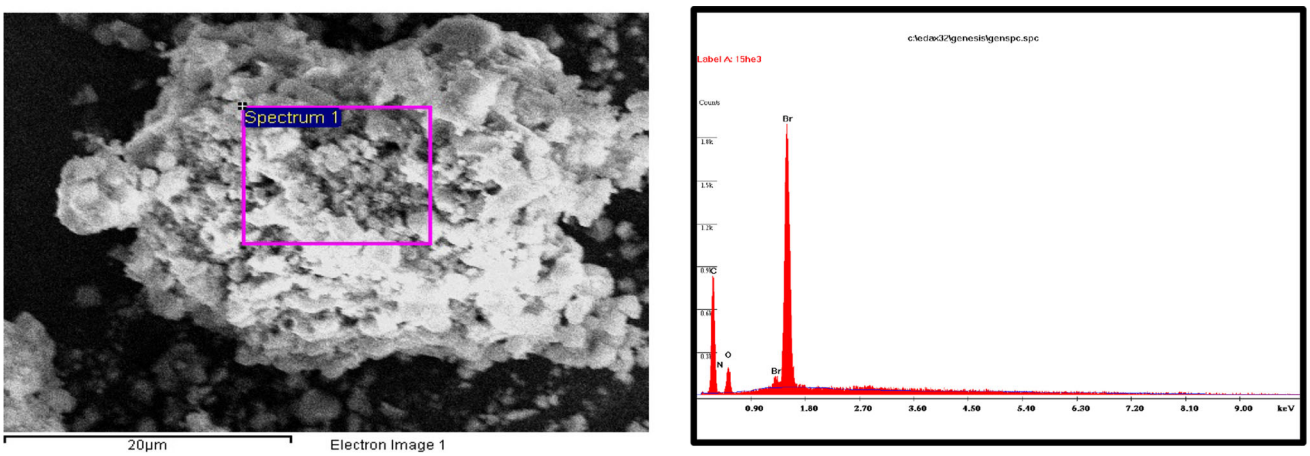

Fig. 7 SEM and EDAX

3.6 Microhardness Studies

Vicker's microhardness test was done by shimadzu HMV-2 with different loads on the well cleaved faces. The static indentation test on such surfaces provides the idea of resistance of material which it offers local deformation or damage under an applied load. The hardness number (H_v) was obtained using the formula $H_v = \frac{1.8544XP}{d^2}$ Kg/mm^2. Where P is the load applied (gm) and d being the diagonal length indentation impression (mm) and the corresponding graph as shown in Fig. 8. it is seen that the observed value of (Hv) raises with increasing applied load for more than 100gm load cracks were to be observed around the indentation and plot a graph of Log p versus Log d to calculate Mayer's index number 'n' and the resulting graph is shown in Fig. 9

The Mayer's number (n) value is greater than 1.6 after the linear fit. Hence, the grown crystal belongs to soft material category. The crystal resistance to deformation by the applied load in terms of stiffness constant (C_{11}) was estimated through the equation $C_{11} = (H_V)^{\frac{7}{4}}$.

The yield strength (σ_v) is a stress from where material originates to wrap plastically and earlier to this position the crystal deform elastically and which can be obtained by the equation

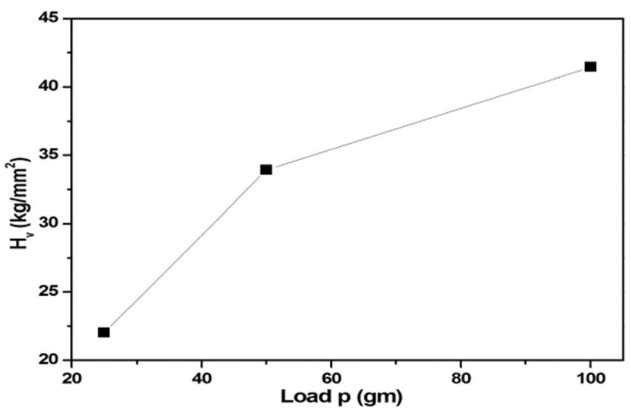

Fig.8 Variation of hardness with load

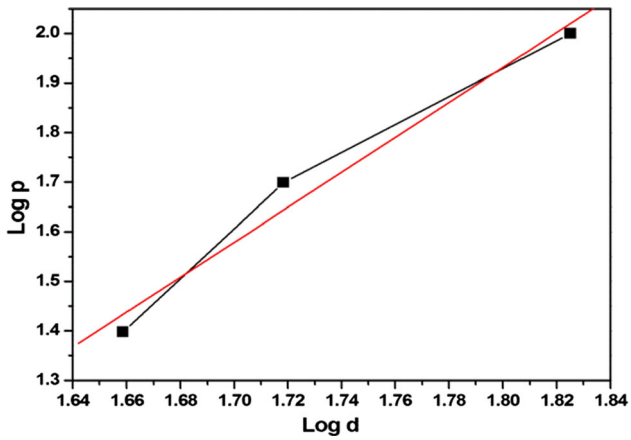

Fig.9 Variation of log p v/s log d

Table 3 Calculated mechanical parameters

Load P(gm)	H_v(kg/mm^2)	σ_v (Gpa)	$C_{11} \times 10^{12}$ Pa
25	22.34	0.936	22.3
50	47.62	1.442	47.6
100	67.71	1.764	67.7

Table 4 SHG efficiency Values of some of the reported L-alanine derivatives

Name of the L-alanine derivative	SHG efficiency value (Relative to KDP)
Pure LAL (Misoguti et al. 1996)	0.33
LAAB (Present work)	0.39
L-alanium oxalate (Dhanuskodi. 2004)	1
L-alanine DL Malic acid (Jaikumar et al. 2009)	0.92
L-alanine admixtured with perchloric acid (Jothi mani et al. 2015)	0.84

$$\sigma_V = \frac{H_V}{2.9}[1-(n-2)]\left(\frac{12.5(n-2)}{1-(n-2)}\right)^{n-2}$$

All the calculated values are tabulated in Table 3.

3.7 Second Harmonic Generation Studies

Being one of the principal methods of measuring NLO features, Kurtz powder method involves the microcrystalline substance on which the laser beam is made to fall resulting in the generation of second harmonic wave. Thus, received beam is filtered and detected and compared with KDP reference. Accordingly, in the present work, Q-switched Nd:YAG LASER having power of 1.9 mJ/pulse was used with. Our sample was well grounded to the identical particle size being 125–150 μm and then taken in the microcapillary. The powder of KDP of same particle size was used for reference. The SHG was proved by the green light emission (wavelength 532 nm), and the efficiency of second harmonic generation is found to be 0.395. The SHG efficiency of few LA derivatives is listed in Table 4.

4 Conclusions

Enviable ammonium bromide doped LA crystals of considerable dimension were successfully grown using aqueous solution. XRD studies revealed its orthorhombic structure. Particle size and strain were evaluated along with slight variation in reflected intensity observation was made from powder diffraction method. From FT-IR, the vibrational frequencies of associated functional groups were confirmed. The crystal has wide optical transmission in the visible and near IR region with lower cut off wavelength of 245 nm. The recorded thermogram revealed that crystal is thermally stable up to 274 °C. The smooth surface of the crystal along with confirmation of dopant in the host was proven by SEM-EDAX studies. The confirmation for the harmonic generation is observed through the green light emission and the SHG efficiency is found to be 0.395 times that of KDP. the dopant in the lattice of host crystal acted as a barrier to the movement of dislocation resulting in the increase in the hardness of the crystal. All these experiential results suggest that the grown crystal can be possible contender for laser associated applications.

Acknowledgements The authors would like to thank the Ministry of education in Saudi Arabia and Taif University Researchers Supporting Project Number (TURSP- 2020/47), Taif University, Taif, Saudi Arabia.

Author Contributions **M. R. H** involved in conceptualization, methodology, article writing, formal analysis, resources, project administration, data curation and investigation. **G. J. S** participated in conceptualization and suggestions given for correction of manuscript, investigation, visualization and editing. **A. A** involved in procurement of resources, materials, characterizations, financial support to completion of this research work and review of the manuscript and editing. **M. R. J** involved in review of manuscript, suggestions given for correction of manuscript, supervision and validation. **B. M. P** participated in assistance in the article writing, resources and software.

Funding None.

Data Availability None.

Declarations

Conflict of interest The authors declare that they have no Conflict of Interest.

References

Arun KJ, Jayalekshmi S (2009) Growth and characterization of nonlinear optical single crystals of L-alaninium oxalate. J Miner Mater Charact Eng 8:635–646. https://doi.org/10.4236/jmmce.2009.88055

Bernal JD (1931) The crystal structure of the natural amino acids and related compounds. Z Kristallogr 78:363–369. https://doi.org/10.1524/zkri.1931.78.1.363

Dhanuskodi S, Vasantha K (2004) Structural, thermal and optical characterizations of a NLO material: L-alaninium oxalate. Cryst Res Technol 39:259–265. https://doi.org/10.1002/crat.200310180

Ding YJ, Mu X, Gu X (2000) Efficient generation of coherent blue and green light based on frequency conversion in $KTiOPO_4$.

J Nonlin Opt Phys Mater. https://doi.org/10.1142/S0218863500000042

Franken PA, Hill AE, Peters CW, Weinreich G (1961) "Generation of optical harmonics." Phys Rev Lett 7:118. https://doi.org/10.1103/PhysRevLett.7.118

Jaikumar D, Kalainathan S, Bhagavanarayana G (2009) Synthesis, growth, thermal, optical and mechanical properties of new organic NLO crystal: L-alanine DL-malic acid. J Cryst Growth 312:120–124. https://doi.org/10.1016/j.jcrysgro.2009.09.056

Krishnakumar V, Nagalakshmi R (2006) Polarised Raman and infrared spectral analysis of l-alanine oxalate (C5H9NO6) a non-linear optical single crystal. Spectrochim Acta A 64:736–743. https://doi.org/10.1016/j.saa.2005.07.074

Lydia Caroline M, Prakash M, Geetha D, Vasudevan S (2011) Growth, structural, vibrational, optical, laser and dielectric aspects of l-alanine alaninium nitrate single crystal. Spectrochimica Acta Part A Mol Biomol Spectrosc 79:1936–1940. https://doi.org/10.1016/j.saa.2011.05.094

Misoguti L, Varela AT, Nunes FD, Bagnato VS, Melo FEA, Mendes Filho J, Zilio SC (1996) Optical properties of L-alanine organic crystals. Opt Mater 6:147–152. https://doi.org/10.1016/0925-3467(96)00032-8

Singh N, Singh BK, Binay Kumar NS (2008) Growth and characterization of new nonlinear optical thiourea L-alanine acetate single crystal. J Cryst Growth 310:4487–4492. https://doi.org/10.1016/j.jcrysgro.2008.07.092

Jothi Mani R, Selvarajan P, Alex Devadoss H, Shanthi D (2015) Second-order, thirdorder NLO and other properties of l-alanine crystals admixture wit perchloric acid (LAPA). Optik 126:213–218. https://doi.org/10.1016/j.ijleo.2014.08.143

Rajan Babu D, Jayaram D, Mohankumar R, Jayavel R (2002) "Growth and characterization of non-linear optical l-alanine tetrafluoroborate (LAlFB) single crystals. J Cryst Growth 245:121–125. https://doi.org/10.1016/S0022-0248(02)01708-6

Rajan Babu D, Jayaraman D, Mohan Kumar R, Jayavel R (2002) Growth and characterization of non-linear optical L-alanine tetrafluoroborate (L-AlFB) single crystals. J Cryst Growth 245:121–125. https://doi.org/10.1016/S0022-0248(02)01708-6

Shanthi D, Selvarajan P, Jothi Mani R (2014) Nucleation kinetics, growth and hardness parameters of l-alanine alaninium picrate (LAAP) single crystals. Optik 125:2531–2537. https://doi.org/10.1016/j.ijleo.2013.10.118

Simpson HJ Jr, Marsh RE (1966) The crystal structure of L-alanine. Acta Crystallogr A 20:550–555. https://doi.org/10.1107/S0365110X66001221

Suresh N, Selvapandiyan M (2020) Growth and multifunctional characteristics of single large crystal derived from pure and 8-hydroxyquinoline-doped L-alanine components. Bull Mater Sci 43:166. https://doi.org/10.1007/s12034-020-02128-0

Wang XQ, Xu D, Yuan DR, Tian YP, Yu WT, Sun SY, Yang ZH, Fang Q, Lu MK, Yan YX, Meng FQ, Guo SY, Zhang GH, Jiang MH (1999) Synthesis, structure and properties of a new nonlinear optical material: zinc cadmium tetrathiocyanate. Mater Res Bull. https://doi.org/10.1016/S0025-5408(99)00211-1